

## Electronic Supplementary Information

### Thermoelectric properties of $\text{CuGa}_{1-x}\text{Mn}_x\text{Te}_2$ : power factor enhancement by the incorporation of magnetic ion

Fahim Ahmed<sup>a,b</sup>, Naohito Tsujii<sup>a</sup> and Takao Mori<sup>a,b</sup>

<sup>a</sup> International Center for Materials Nanoarchitectonics (MANA), National Institute for Materials Science (NIMS), Namiki 1-1, Tsukuba 305-

0044, Japan. E-mail: TSUJII.Naohito@nims.go.jp; MORI.Takao@nims.go.jp

<sup>b</sup> Graduate School of Pure and Applied Sciences, University of Tsukuba, 1-1-1 Tennodai, Tsukuba, Ibaraki 305-8577, Japan

#### 1. Schematic structure of Chalcopyrite $\text{CuGaTe}_2$ .

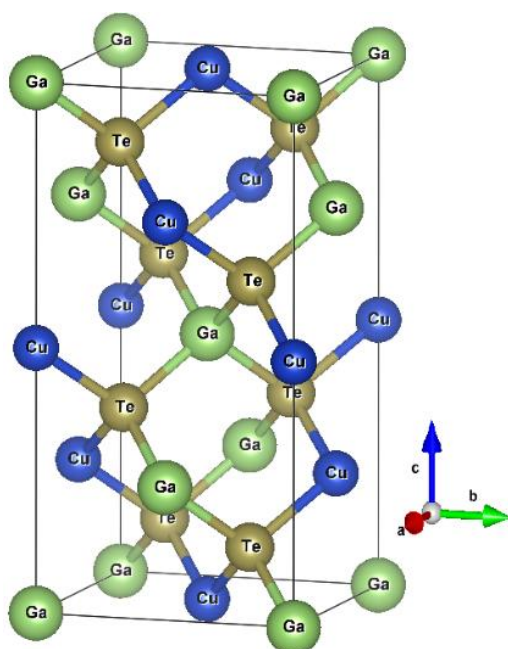


Fig. S1 Structure of chalcopyrite shown along vertical  $c$  axis.

## 2. Rietveld Refinement.

Rietveld refinement was done for structural analysis by using FullProf Suite software<sup>1</sup> on all synthesized samples as shown in Fig S2. Tripled pseudo-Voigt function was employed to analyze the peak shape. Bragg positions are shown on black line which agreed with synthesized structure peaks. Refinement results show single phase chalcopyrite structure for all samples.

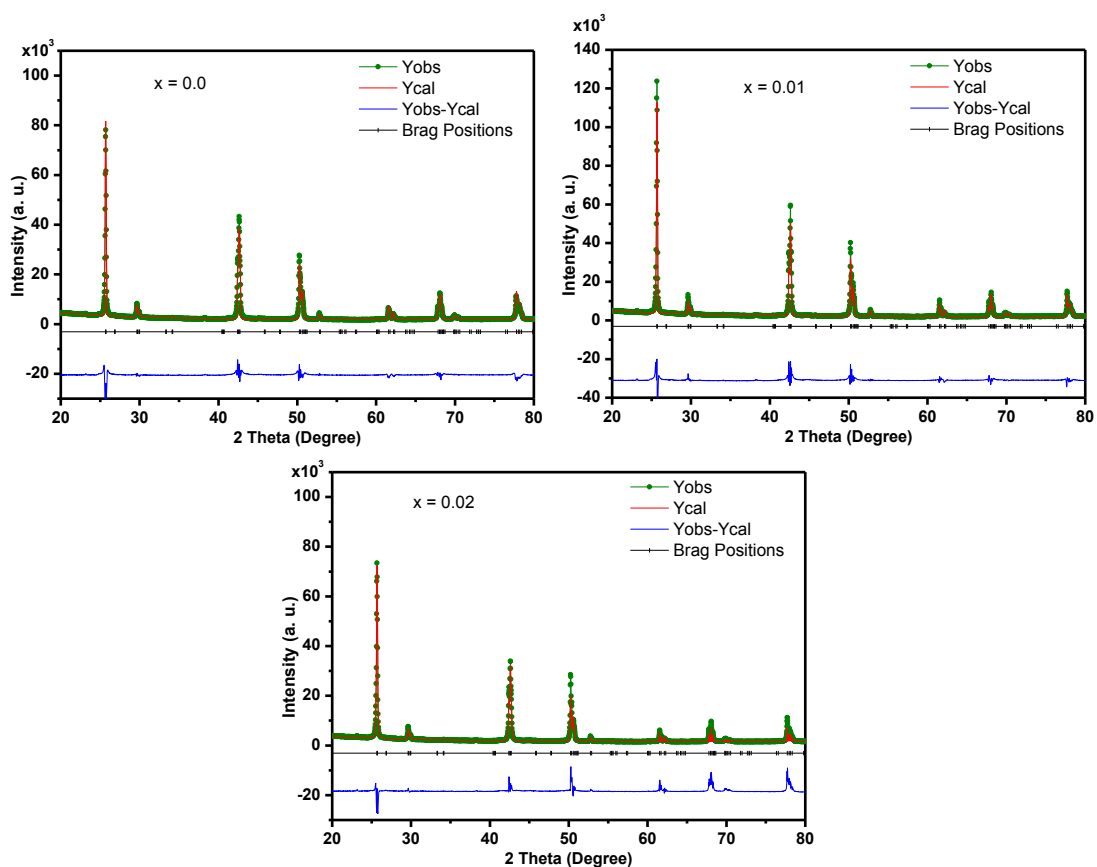


Figure S2. Results of Rietveld refinement for the  $\text{CuGa}_{1-x}\text{Mn}_x\text{Te}_2$ ,  $x = 0.0, 0.01, 0.02$  including the observed and calculated diffraction data along with their difference.

### 3. Thermal Conductivity.

Lattice thermal conductivity ( $\kappa_{lat}$ ) and thermal conductivity due to charge carriers ( $\kappa_{elec}$ ) are two main terms which are generally considered for explaining total thermal conductivity ( $\kappa_{tot}$ ) and are related as<sup>2</sup>

$$\kappa_{tot} = \kappa_{lat} + \kappa_{elec}$$

Where  $\kappa_{elec}$  can be evaluated by using Wiedemann-Franz law<sup>3</sup>  $\kappa_{tot} = L\sigma T$  where  $L$ ,  $\sigma$  and  $T$  are Lorentz number, electrical conductivity and temperature respectively. For better thermal transport analysis, electronic and lattice contributions were evaluated as shown in Fig S3. Electronic thermal conductivity increases gradually with an increase in temperature but overall percentage towards total thermal conductivity is minor as compared to lattice thermal conductivity. Hence at higher temperatures scattering of phonons lead to decrease in total thermal conductivity of samples.

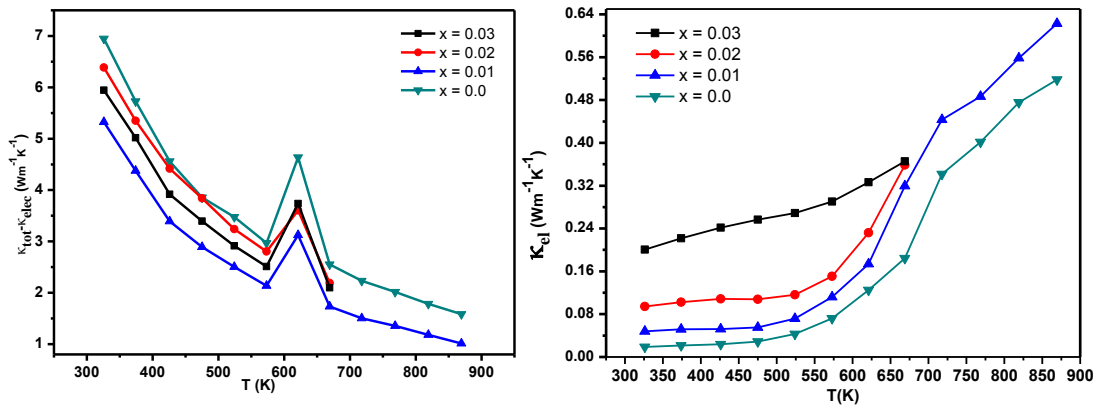


Figure S3 Temperature dependence of (a) Lattice thermal conductivity  $\kappa_{lat} = \kappa_{tot} - \kappa_{elec}$ , and (b) Electronic thermal conductivity  $\kappa_{elec}$ .

#### 4. Seebeck Coefficients.

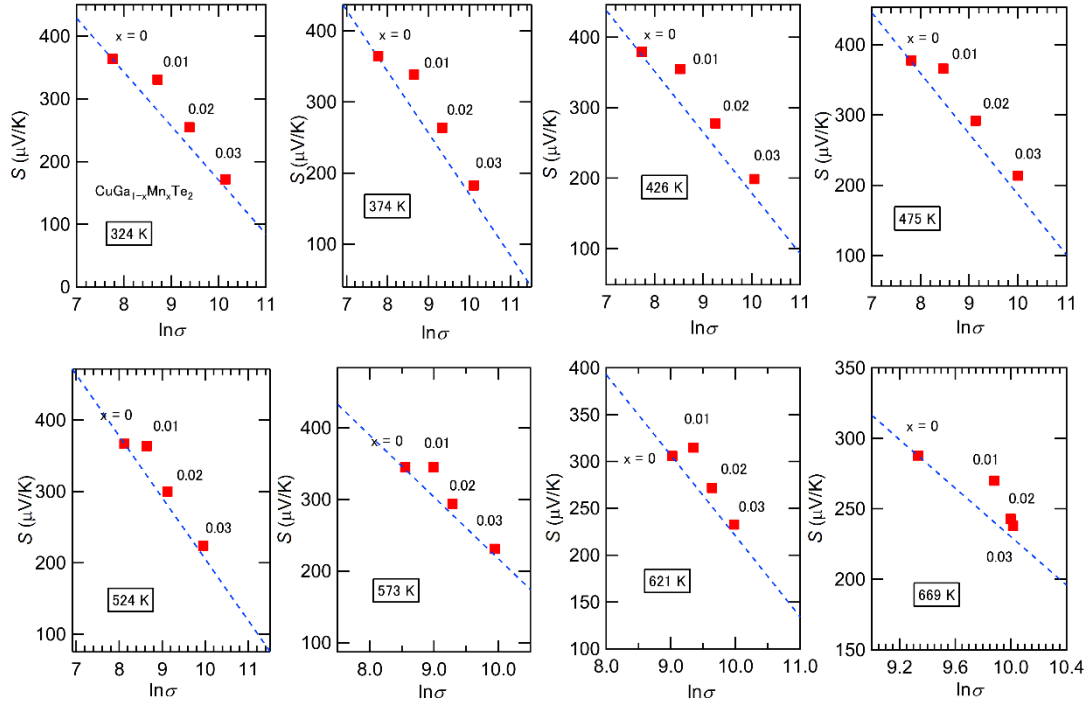


Fig. S4 Plots of Seebeck coefficient  $S$  and  $\ln\sigma$  for  $\text{CuGa}_{1-x}\text{Mn}_x\text{Te}_2$ . Broken lines have the slope of -86.14  $\mu\text{V/K}$  as suggested by Rowe and Min<sup>4</sup>.

## 5. Power Factor.

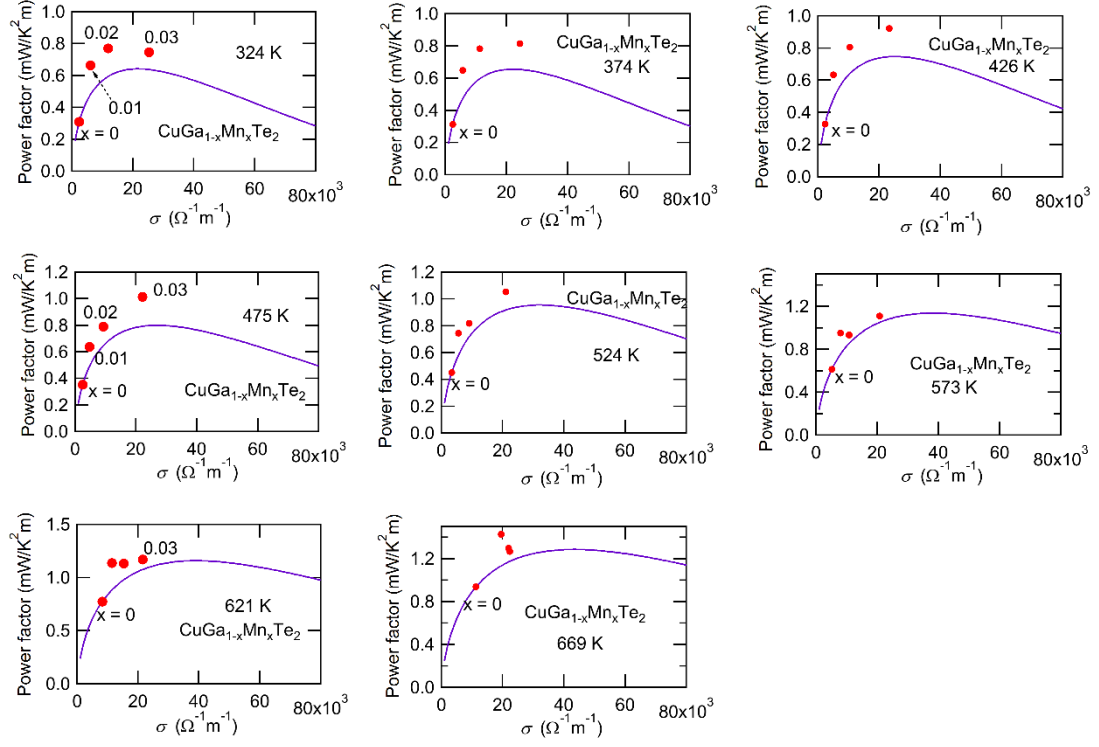


Fig. S5 Power factors  $S^2\sigma$  of CuGa<sub>1-x</sub>Mn<sub>x</sub>Te<sub>2</sub> as functions of electrical conductivity  $\sigma$ . Solid lines are the calculation based on the theoretical model<sup>4</sup> with the values of  $x = 0$  obtained by our measurements. Filled circles show the values for  $x = 0, 0.01, 0.02, 0.03$  observed in the present work.

## 6. Magnetic data

$x$	$C$ (emu K/mol)	$p_{\text{eff}}/\mu_{\text{B}}$	$\theta$ (K)
0.01	0.0344	5.24	-59.1
0.02	0.0788	5.61	-129.0
0.03	0.1073	5.35	-108.5

Table S1. Magnetic parameters obtained by the Curie-Weiss fitting of the magnetic susceptibility data of  $\text{CuGa}_{1-x}\text{Mn}_x\text{Te}_2$ .

## 7. Seebeck coefficient at low temperature

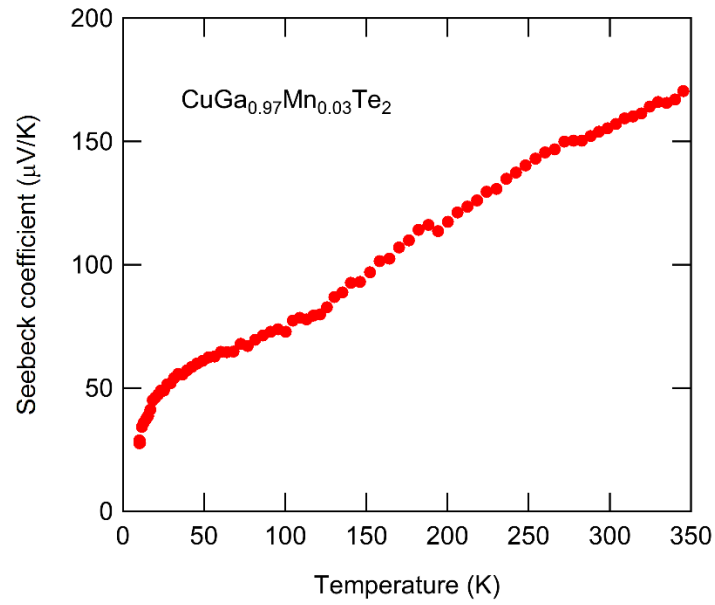


FIG. S6 Seebeck coefficient of  $\text{CuGa}_{0.97}\text{Mn}_{0.03}\text{Te}_2$  at low temperature.

## 6. References

- 1- J. Rodrigues-Carvajal, 1993 *Physica B*, **192**, 55
- 2- J-P. Issi, J. Heremans, *Physical Review B* 1983 **27**, 1333
- 3- H. Ning, G. D. Mastrorillo, S. Grasso, B. Du, T. Mori, C. Hu, Y. Xu, K. Simpson, G. Maizza, M. J. Reece, *J. Mater. Chem. A*, 2015, **3**, 17426
- 4- M. Rowe, G. Min, *J. Mater Sci Lett*, 1995, **14**, 617